Electronic Supplementary Information

Integrating lignin depolymerization with microbial funneling processes using agronomically relevant feedstocks

Jose M. Perez,[§a,b,c] Canan Sener,[§b,c] Shamik Misra,[§c,d] German E. Umana,[a,b,c] Jason Coplien,[b,c] Dennis Haak,[b,c] Yanding Li,[b,c] Christos T. Maravelias,[d,e] Steven D. Karlen,[b,c] John Ralph,[b,c,f] Timothy J. Donohue,[b,c,g] Daniel R. Noguera*[a,b,c]

[a.] Department of Civil and Environmental Engineering, University of Wisconsin-Madison, Madison, Wisconsin 53706.

[b.] Wisconsin Energy Institute, University of Wisconsin-Madison, Madison, Wisconsin 53726.

[c.] Great Lakes Bioenergy Research Center, University of Wisconsin-Madison, Madison, Wisconsin 53726.

[d.] Andlinger Center for Energy and the Environment, Princeton University, Princeton, NJ, 08544.

[e.] Department of Chemical and Biological Engineering, Princeton University, Princeton, New Jersey 08544

[f.] Department of Biochemistry, University of Wisconsin-Madison, Madison, Wisconsin 53726.

[g.] Department of Bacteriology, University of Wisconsin-Madison, Madison, Wisconsin 53706.

[§]These authors equally contributed to this work.

*Corresponding author: Daniel R. Noguera, noguera@engr.wisc.edu

Supplemental Figures and Tables

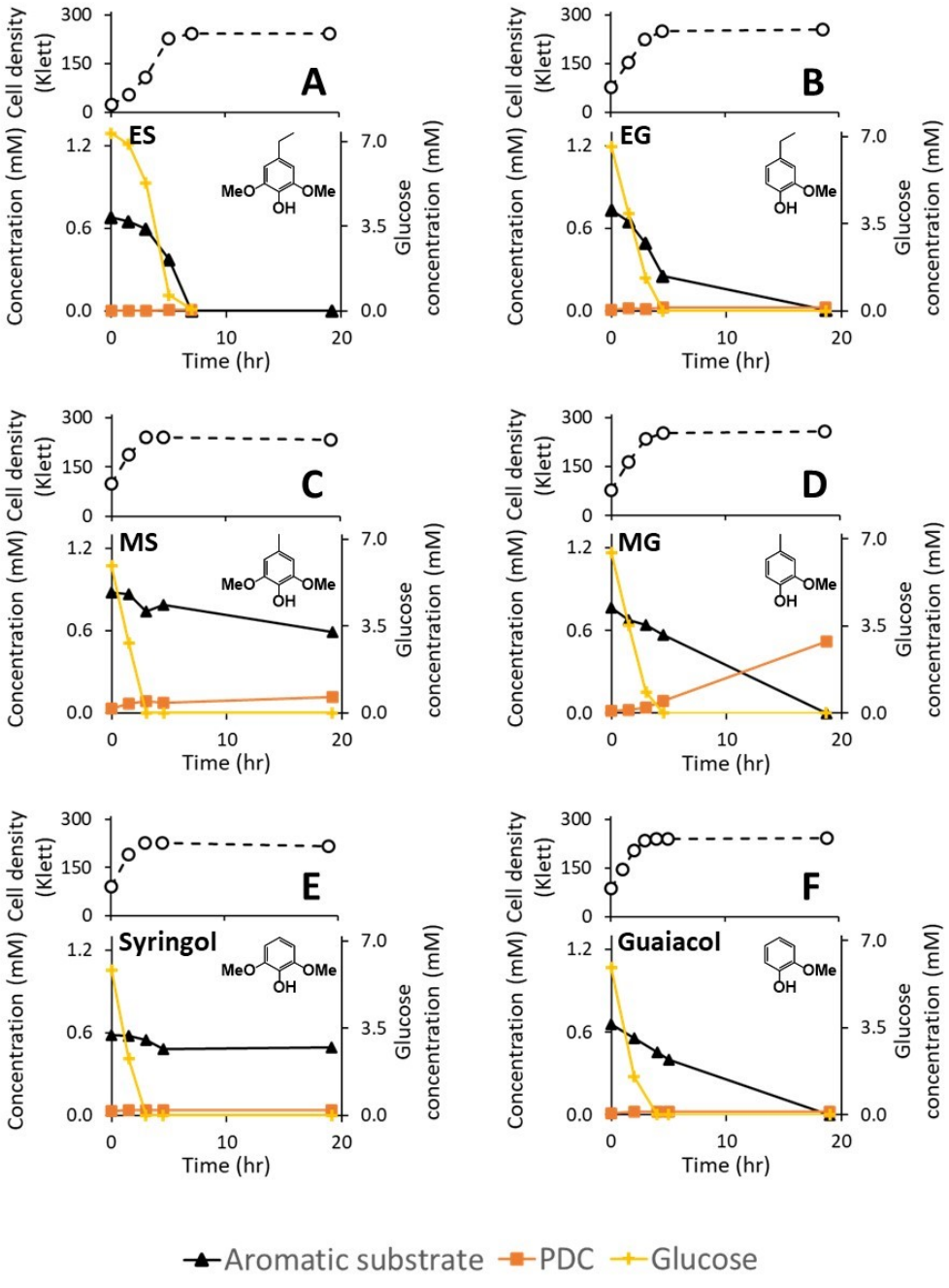

Figure S1. Cell density and extracellular metabolite concentration of *N. aromaticivorans* strain PDC cultures in minimum media supplemented with glucose and ethylsyringol (ES) (A), ethylguaiacol (EG) (B), methylsyringol (MS) (C), methylguaiacol (MG) (D), syringol (E), or guaiacol (F). Values correspond to the average of three biological replicates.

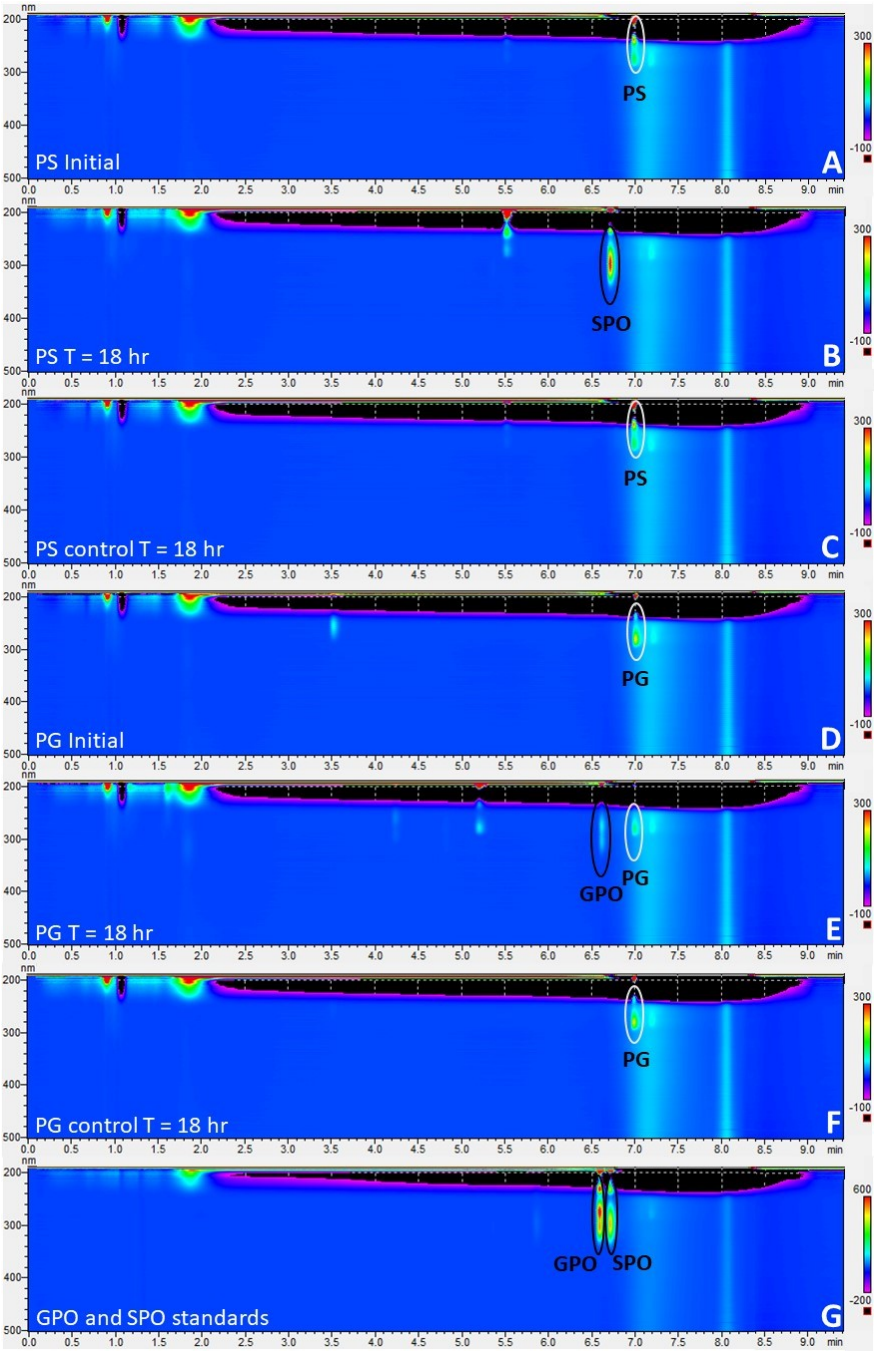

Figure S2. UV/vis chromatogram of samples from experiments with PS and PG collected at the beginning of the experiment (A and D, respectively), after 18 hours (B and E), from an abiotic control after 18 h of incubation (C and F), and authentic standards of 3,5-dimethoxy-4-hydroxyphenylpropanone (SPO) and 4-hydroxy-3-methoxyphenylpropanone (GPO) (G). PS completely disappeared and PG partially disappeared after 18 h of experiment with *N. aromaticivorans* strain PDC; SPO and GPO were detected in experiments supplemented with PS and PG, respectively. Abiotic controls showed the presence of PS (C) and PG (F), and the absence of new peaks after 18 h of incubation.

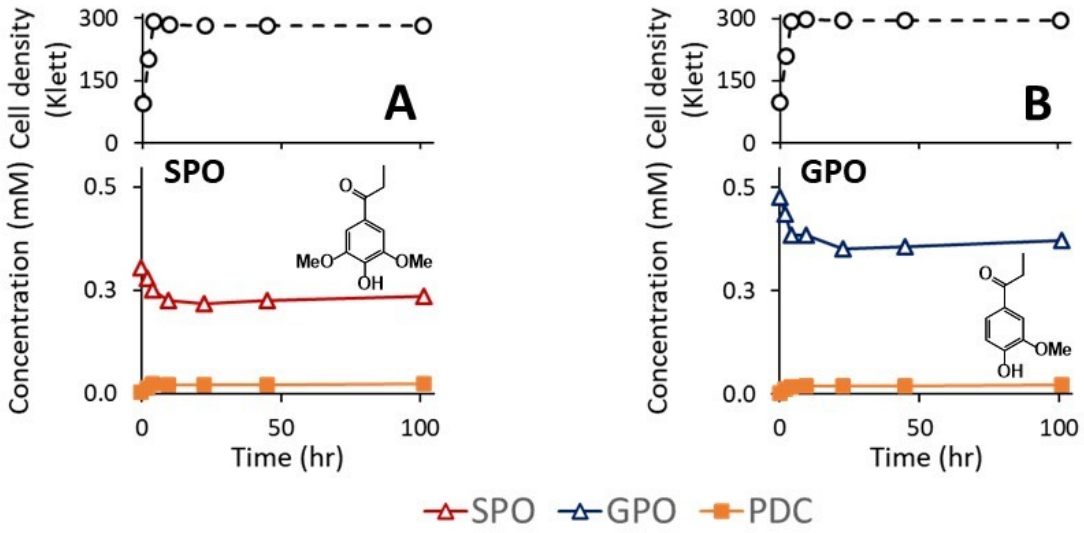

Figure S3. Cell density and extracellular metabolite concentration of *N. aromaticivorans* strain PDC cultures in minimum media supplemented with glucose and 3,5-dimethoxy-4-hydroxyphenylpropanone (SPO) (A) or 4-hydroxy-3-methoxyphenylpropanone (GPO) (B). Values correspond to the average of three biological replicates.

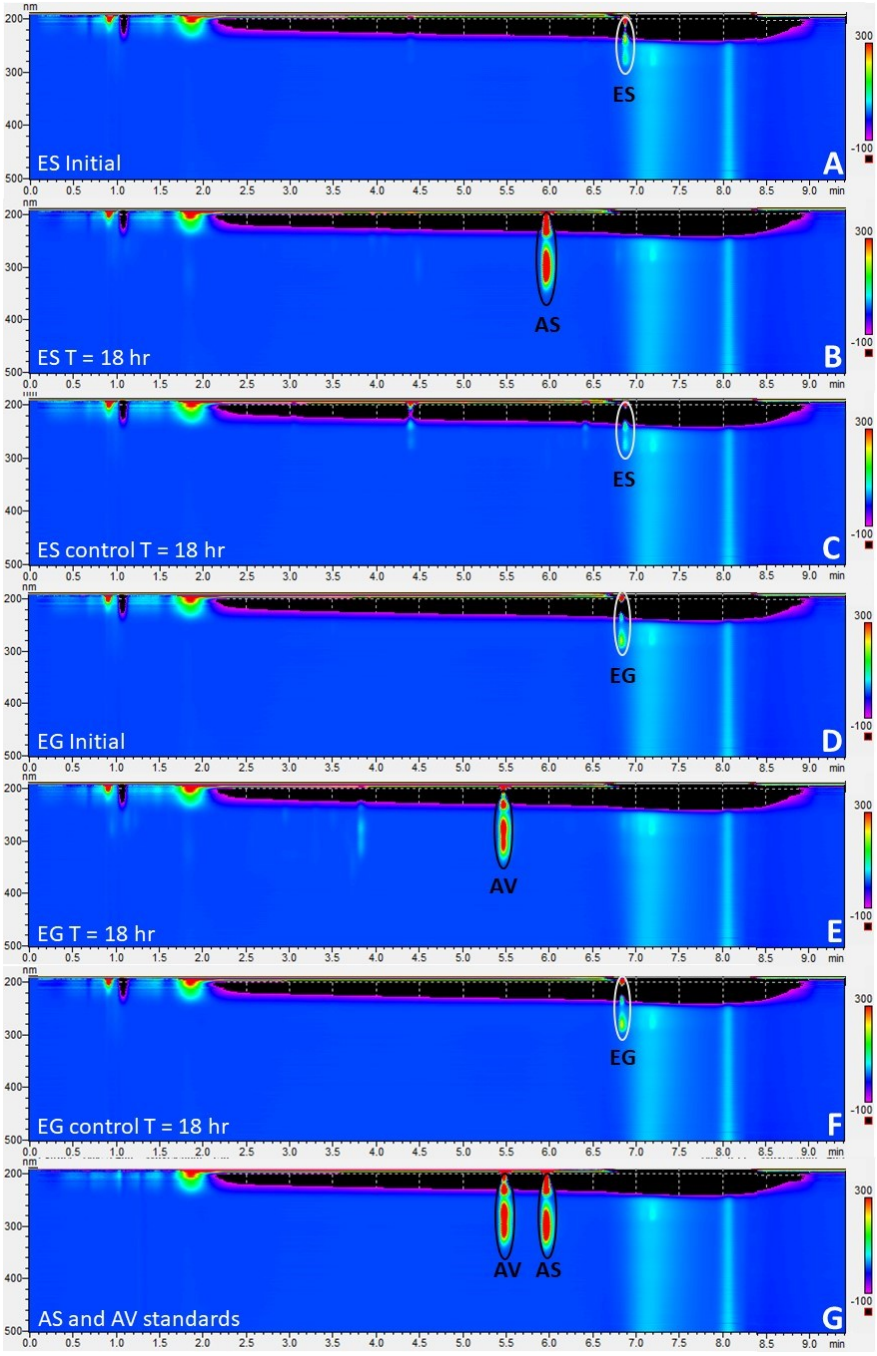

Figure S4. UV/vis chromatogram of samples from experiments with ES and EG collected at the beginning of the experiment (A and D, respectively), after 18 h (B and E), from an abiotic control after 18 h of incubation (C and F), and authentic standards of acetosyringone (AS) and acetovanillone (AV) (G). ES and EG completely disappeared after 18 h of experiment with *N. aromaticivorans* strain PDC; AS and AV were detected in experiments supplemented with PS and PG, respectively. Abiotic controls showed the presence of ES (C) and EG (F), and the absence of new peaks after 18 h of incubation.

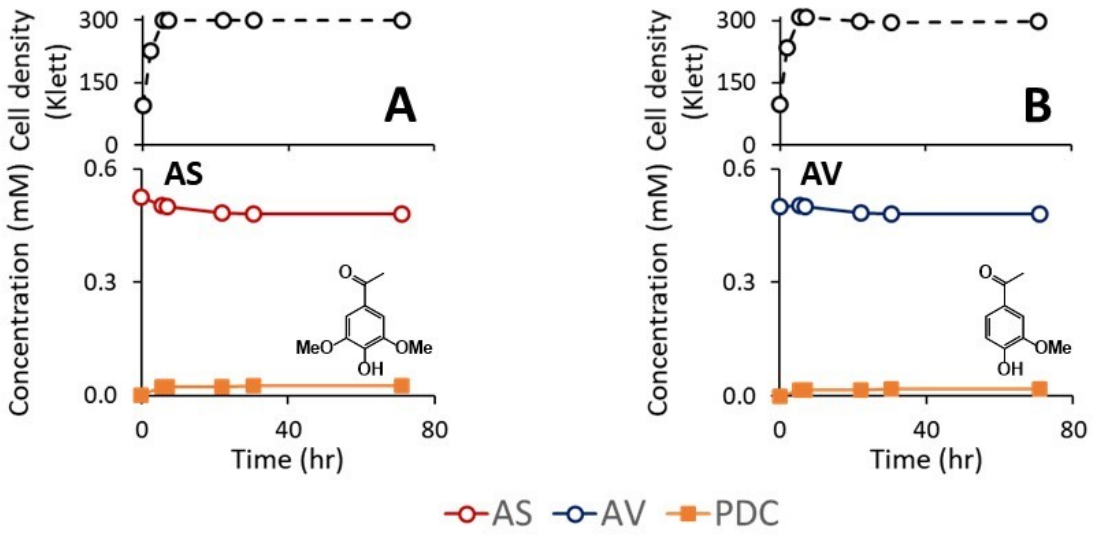

Figure S5. Cell density and extracellular metabolite concentration of *N. aromaticivorans* strain PDC cultures in minimum media supplemented with glucose and acetosyringone (AS) (A) or acetovanillone (AV) (B). Values correspond to the average of three biological replicates.

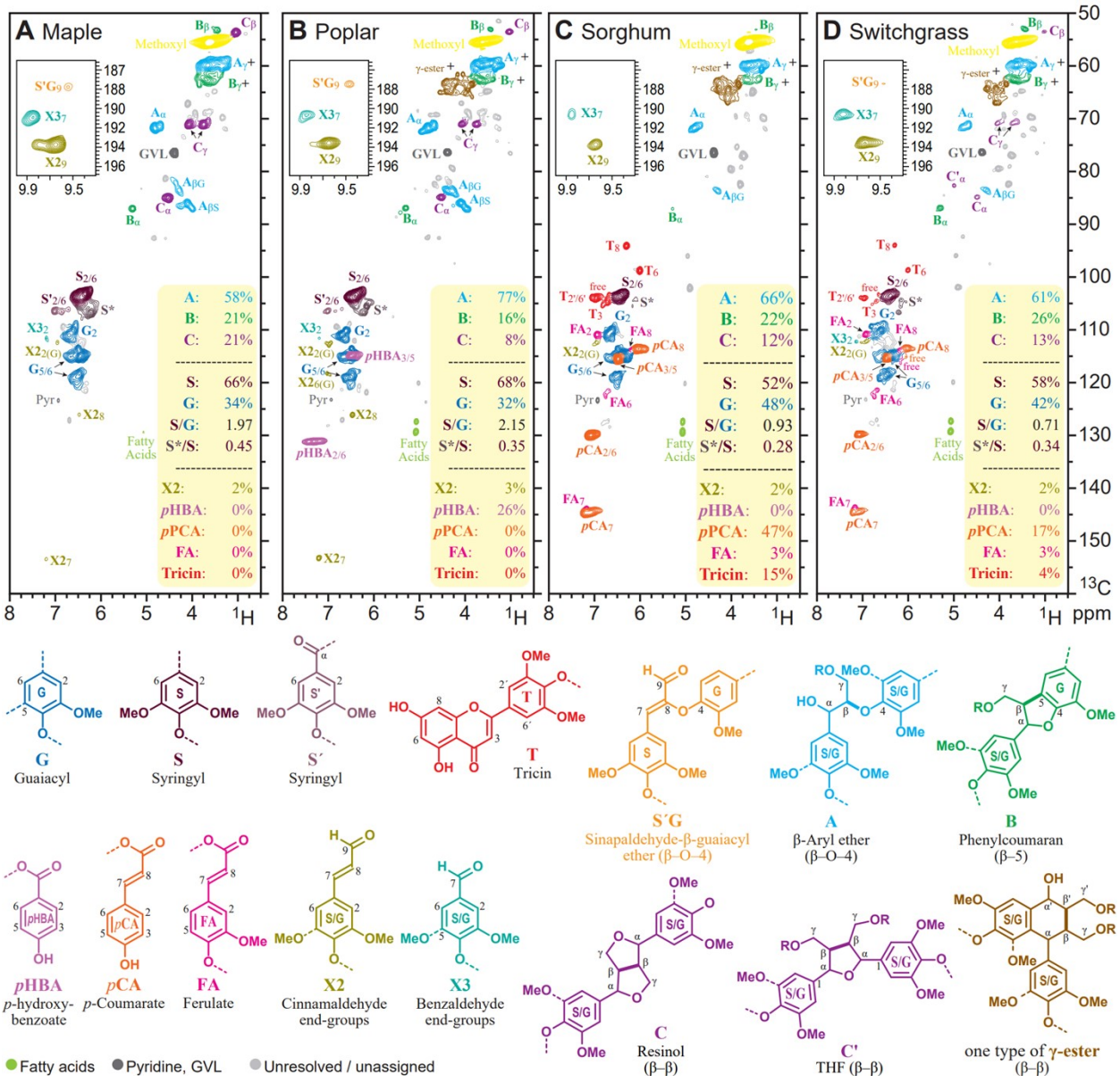

Figure S6. (**A-D**) Short-range ^{1}H–^{13}C correlation (HSQC) NMR spectra of isolated lignins used in the hydrogenolysis experiments. Volume-integrals are given for the lignin aromatic and substructure units that are labeled and color-coded to match their assignments in the spectrum. The aromatic percentages are on a [$0.5*S_{2/6}+G_2=100\%$] basis and the sidechains percentages are on a [$A_\alpha+B_\alpha+0.5*9(C_\alpha+C'_\alpha)=100\%$] basis. The signals corresponding to S* are assigned as condensed S-units and provide, when converted to a ratio of S*/S, an indication of lignin condensation.

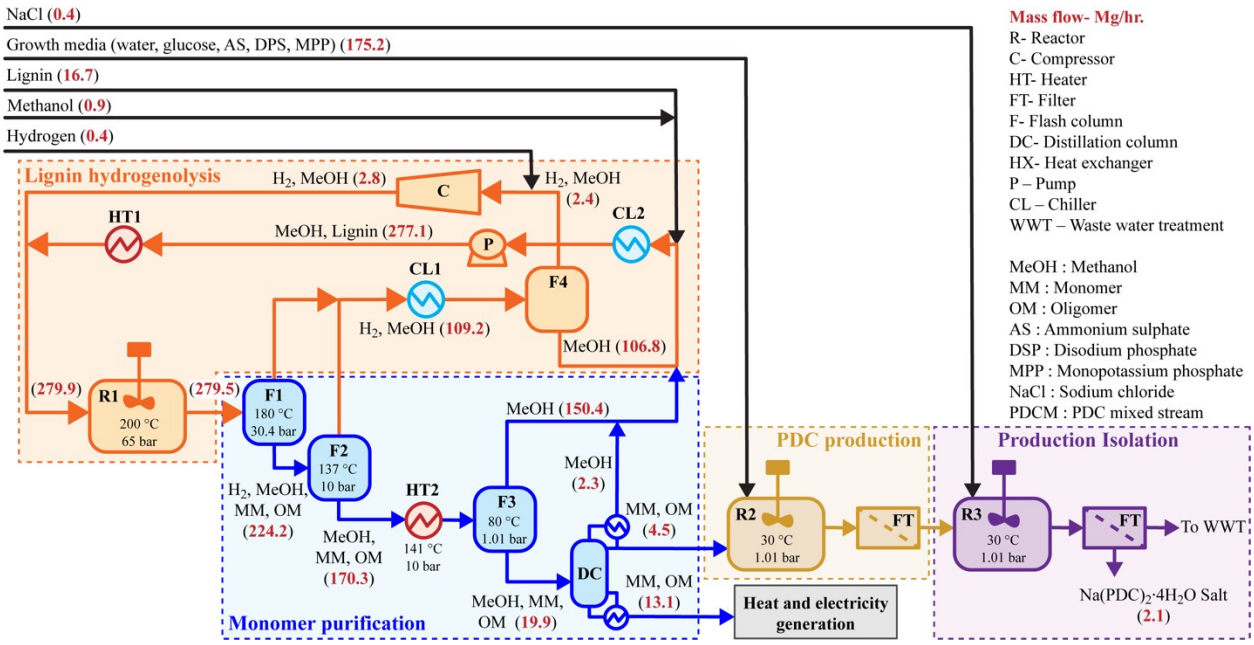

Figure S7. Detailed process flow-diagram of the simulated lignin-to-PDC biorefinery showing all the unit processes.

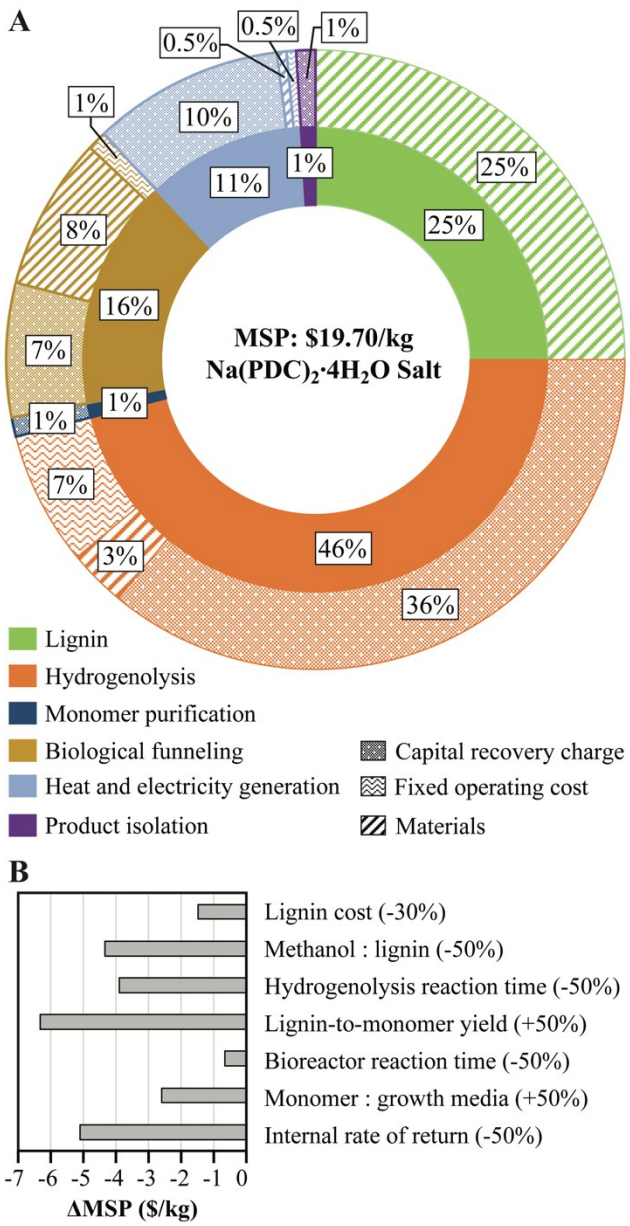

Figure S8. Technoeconomic analysis of case that considers reactor with thick walls potentially needed for the hydrogenolysis section of the biorefinery, based on Bartling et al.[1]. (A) Circular diagram showing in the inner circle the contribution of six sections to the minimum selling price of PDC and in the outer circle the contribution of capital cost, materials, and fixed operational cost to each of the simulated sections. (B) Sensitivity analysis showing change in MSP after changing the shown parameter by a percent indicated in parenthesis.

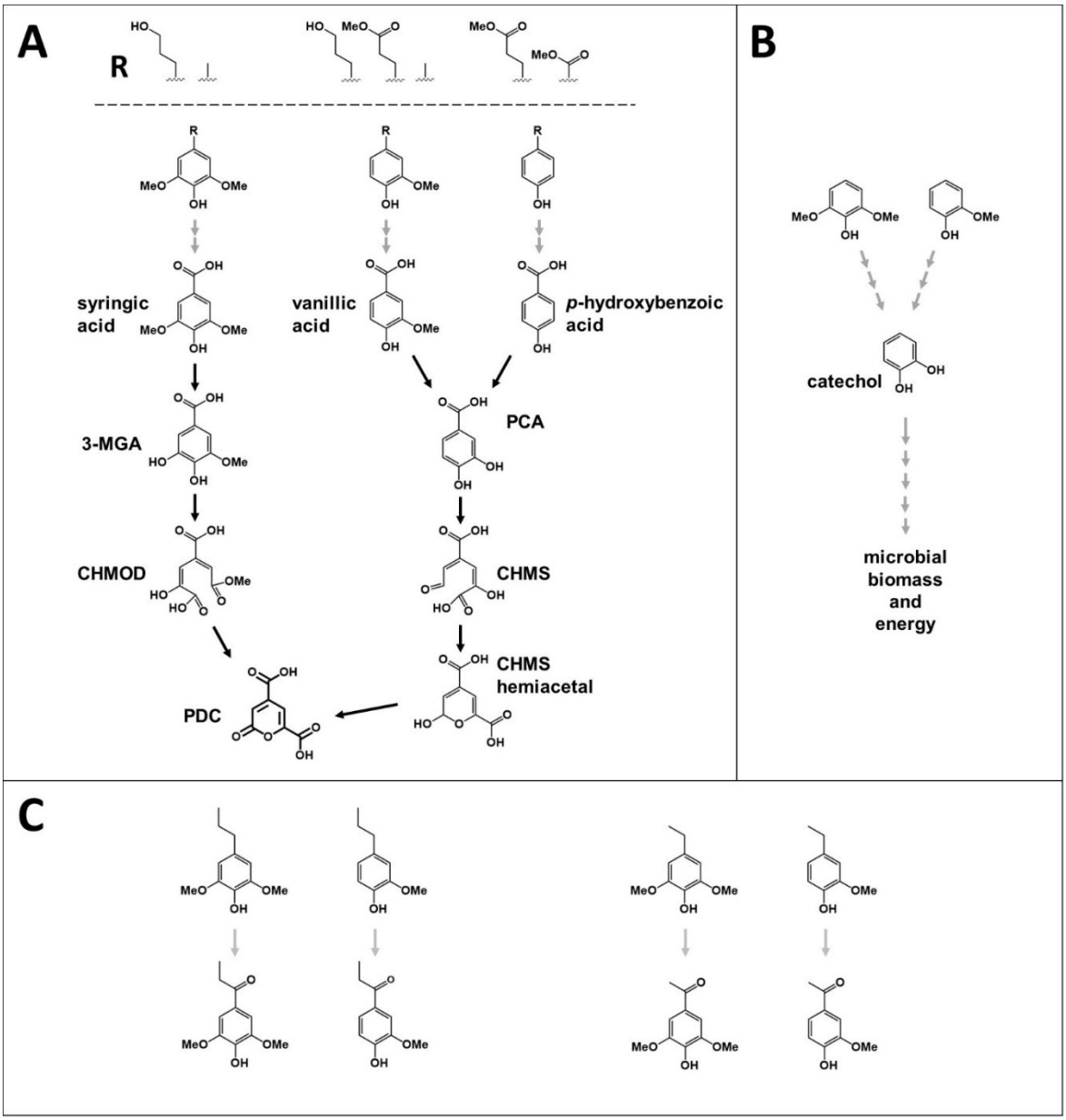

Figure S9. Metabolic pathways for degradation of aromatic compounds by *N. aromaticivorans*. (A) Aromatic compounds that produced PDC with the engineer *N. aromaticivorans* PDC strain are catalyzed through the central pathways for degradation of syringic acid, vanillic acid, and *p*-hydroxybenzoic acid.[2] Black arrows show steps with confirmed enzymatic reactions, and grey arrows show proposed reactions for which enzymes have not been identified. (B) Guaiacol is degraded via catechol and does not enter the central pathways that produce PDC. (C) Syringols and guaiacols with propyl and ethyl sidechains are oxidized, forming aryl ketones that are not further degraded. Abbreviations: 3-methylgallate, 3-MGA; 4-carboxy-2-hydroxy-6-methoxy-6-oxohexa-2,4-dienoate, CHMOD; 2-pyrone-4,6-dicarboxylic acid, PDC; protocatechuic acid (PCA); 4-carboxy-2-hydroxy-*cis,cis*-muconate-6-semialdehyde, CHMS.

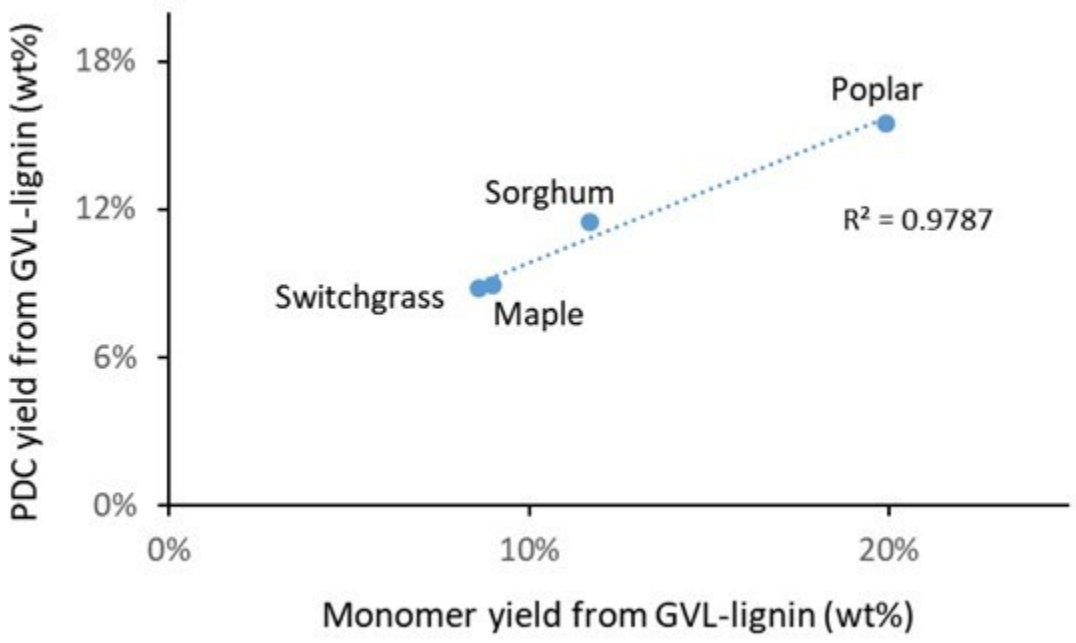

Figure S10. Lignin to monomer yield (wt%) v/s lignin to PDC yield (wt%) for maple, poplar, sorghum, and switchgrass.

Table S1. Concentration of aromatic substrates measured at the beginning and at the end of experiments supplemented with 7,8-dihydrosinapyl alcohol (DSA), 7,8-dihydroconiferyl alcohol (DCA), 7,8-dihydroferulic acid methyl ester (Me-DHFA), 7,8-dihydro-*p*-coumaric acid methyl ester (Me-DH*p*CA), *p*-hydroxybenzoic acid methyl ester (Me-*p*HBA), propylsyringol (PS, syringylpropane), and propylguaiacol (PG, guaiacylpropane)

	Initial concentration (mM)	**Final concentration (mM)**
DSA	0.83	0.00
DCA	0.98	0.00
Me-DHFA	0.90	0.00
Me-DHpCA	0.79	0.00
Me-*p*HBA	0.67	0.35
PS	0.75	0.00
PG	1.18	0.51

Table S2. Ratio of quantified hydrogenolysis monomers determined by GC-FID analysis of the crude filtered methanol product solution.

Monomer	Maple	Poplar	Sorghum	Switchgrass
Propylsyringol (PS)	2.7%	14.0%	5.6%	5.5%
7,8-Dihydrosinapyl alcohol (DSA)	39.1%	35.8%	9.6%	13.2%
Methylsyringol (MS)	4.3%	1.6%	0.7%	1.2%
Syringol	2.0%	1.0%	0.5%	0.6%
Propylguaiacol (PG)	2.0%	1.4%	2.1%	1.6%
7,8-Dihydroconiferyl alcohol (DCA)	32.9%	26.0%	12.9%	22.2%
7,8-dihydroferulic acid methyl ester (Me-DHFA)	0.2%	0.3%	8.6%	11.3%
Ethylguaiacol (EG)	4.7%	2.2%	3.1%	4.9%
Methylguaiacol (MG)	3.4%	0.9%	1.2%	2.3%
Guaiacol	0.8%	0.2%	0.6%	0.8%
Propylphenol (PH)	3.5%	3.7%	6.9%	7.6%
7,8-Dihydro-*p*-hydroxycinnamyl alcohol (DHA)	2.8%	1.3%	0.3%	0.6%
7,8-dihydro-*p*-coumaric acid methyl ester (Me-DH*p*CA)	1.1%	0.4%	44.7%	26.0%
p-hydroxybenzoic acid methyl ester (Me-*p*HBA)	0.3%	11.0%	3.1%	2.2%

Table S3. Concentration of aromatic substrates measured at the beginning and at the end of experiments supplemented with depolymerized lignin from maple, poplar, sorghum, and switchgrass

	Maple		Poplar		Sorghum		Switchgrass	
	Initial (mM)	Final (mM)	Initial (mM)	Final (mM)	Initial (mM)	Final (mM)	Initial (mM)	Final (mM)
DSA	0.0470	0.000	0.0941	0.000	0.0161	0.000	0.0157	0.000
DCA	0.0377	0.000	0.0682	0.000	0.0214	0.000	0.0265	0.000
Me-DHFA	0.0003	0.000	0.0008	0.000	0.0144	0.000	0.0135	0.000
Me-DH*p*CA	0.0012	0.000	0.0009	0.000	0.0746	0.000	0.0310	0.000
Me-*p*HBA	0.0004	0.000	0.0288	0.000	0.0051	0.000	0.0026	0.000
*p*HBA	0.0000	0.000	0.0170	0.000	0.0000	0.000	0.0000	0.000
PS	0.0033	0.000	0.0366	0.000	0.0093	0.000	0.0066	0.000
PG	0.0024	0.000	0.0038	0.000	0.0035	0.000	0.0019	0.000
ES	0.0000	0.000	0.0000	0.000	0.0000	0.000	0.0000	0.000
EG	0.0056	0.000	0.0059	0.000	0.0052	0.000	0.0059	0.000
MS	0.0051	0.000	0.0043	0.000	0.0012	0.000	0.0014	0.000
MG	0.0039	0.000	0.0024	0.000	0.0021	0.000	0.0027	0.000
Syringol	0.0024	0.000	0.0026	0.000	0.0008	0.000	0.0007	0.000
Guaiacol	0.0009	0.000	0.0006	0.000	0.0010	0.000	0.0009	0.000

Table S4. List of economic parameters and assumptions

Hydrogen ($ per ton)[a]	1432
Methanol ($ per ton)[b]	389
Freshwater ($ per ton)[a]	0.5
Glucose ($ per ton)[a]	791
Disodium phosphate ($ per ton)[c]	1000
Monopotassium phosphate ($ per ton)[c]	900
Ammonium sulfate ($ per ton)[d]	281
5 wt. % Pd/C Catalyst ($ per ton)[c]	100000
Electricity ($ per kwh)[e]	0.683
Natural gas ($ per ton)[a]	256
Cooling water ($ per MJ)[f]	2.38e-04
Fired heat ($ per MJ)[f]	4.8e-03
Disposal of ash ($ per ton)[g]	36.7
Boiler chemicals ($ per ton)[g]	5994
Plant operating hours per year [a]	7880
Plant life (year)[a]	30
Internal rate of return (%)*[h]	30
Plant depreciation (year)[a]	7
Loan terms (year)[a]	10
Tax rate (%)[a]	35

* Internal rate of return is assumed as 30% to reflect the higher risk in investing new technology.[3]

Assumptions:

- Capital investment is spread over three years at a rate of 8%, 60%, and 32% in the first, second, and third years, respectively.
- Working capital is 5% of fixed capital investment.
- All the costs reported above are adjusted to 2019 $ value.
- Total direct cost (TDC) = 117.5% of the installed cost (IC).
- Total indirect cost (TIC) = 60% of TDC
- Working capital = 5% of the fixed capital investment (FCI = TDC+TIC)
- Maintenance cost= 3% of the IC
- Labor cost= 1.6% of the IC
- Property insurance and tax = 0.7% of the FCI

[a] Taken from Davis et al.[4]

[b] Taken from Liao et al.[5]

[c] Taken from Alibaba[6]

[d] Taken from Intratec[7]

[e] Taken from EIA[8]

[f] Estimated from Aspen Process Economic Analyzer (V10 Aspen Technology)

[g] Taken from Davis et al.[9]

[h] Taken from Alonso et al.[3]

Table S5. MRM transitions used to quantify aromatic monomers in the *N. aromaticivorans* bioconversion assays.

Mass Spectrometer	**Shimadzu LCMS-8045**									
ESI Source	300 °C Ionization mode: DUIS ESI/APCI									
Operation Mode	Multiple Reaction Monitoring (MRM) Argon gas, 230 kPa									
MRM Transition Details Positive (+) mode										
Compound Name	**Retention Time**	**Transition 1**	**CE 1**	**Rel. int.**	**Transition 2**	**CE 2**	**Rel. int.**	**Transition 3**	**CE 3**	**Rel. int.**
Guaiacol	4.84 min	125>65	-21	100	125>93	-15	75			
7,8-Dihydroconiferyl alcohol (DCA)	4.92 min	183>137	-13	100	183>133	-12	45	183>105	-20	45
7,8-Dihydrosinapyl alcohol (DSA)	5.30 min	213>195	-20	100	213>167	-13	81	213>107	-6	46
Syringol	5.49 min	155>123	-23	144	155>95	-30	100	155>77	-45	72
p-Hydroxybenzoic acid methyl ester (Me-*p*HBA)	6.09 min	153>121	-20	100	153>93	-25	48	153>65	-32	62
Methylguaiacol (MG)	6.33 min	139>107	-15	100	139>79	-20	87	139>77	-26	55
7,8-Dihydro-*p*-coumaric acid methyl ester (Me-DH*p*CA)	6.4 min	181>107	-26	100	181>149	-10	0			
Methylsyringol (MS)	6.58 min	169>137	-26	100	169>109	-32	80	169>91	-40	72
Ethylsyringol (ES)	6.61 min	183>65	-32	100	183>95	-35	90	183>91	-14	88
7,8-Dihydro-ferulic acid methyl ester (Me-DHFA)	6.62 min	211>137	-20	100	211>179	-9	48	211>122	-34	22
Ethylguaiacol (EG)	6.88 min	153>77	-26	100	153>121	-15	97	153>91	-23	46
Propylguaiacol (PG)	7.05 min	167>125	-14	100	167>107	-16	184	167>135	-13	99
Propylsyringol (PS)	7.05 min	197>123	-18	100	197>79	-47	31	197>107	34	26
MRM Transition Details Negative (-) mode										
PDC	1.44 min	183>111	13	100	183>139	11	95	183>95	11	67
p-Hydroxybenzoic acid (*p*HBA)	2.68 min	137>93	14	100	137>65	29	10			

References

1. A. W. Bartling, M. L. Stone, R. J. Hanes, A. Bhatt, Y. Zhang, M. J. Biddy, R. Davis, J. S. Kruger, N. E. Thornburg, J. S. Luterbacher, R. Rinaldi, J. M. Samec, B. F. Sels, Y. Román-Leshkov and G. T. Beckham, *Energy Environ. Sci.*, 2021, **14**, 4147-4168.
2. J. M. Perez, W. S. Kontur, M. Alherech, J. Coplien, S. D. Karlen, S. S. Stahl, T. J. Donohue and D. R. Noguera, *Green Chem.*, 2019, **21**, 1340-1350.
3. D. M. Alonso, S. H. Hakim, S. Zhou, W. Won, O. Hosseinaei, J. Tao, V. Garcia-Negron, A. H. Motagamwala, M. A. Mellmer, K. Huang, C. J. Houtman, N. Labbé, D. P. Harper, C. Maravelias, T. Runge and J. A. Dumesic, *Sci. Adv.*, 2017, **3**, e1603301.
4. R. Davis, N. Grundl, L. Tao, M. J. Biddy, E. C. D. Tan, G. T. Beckham, D. Humbird, D. N. Thompson and M. S. Roni, Process design and economics for the conversion of lignocellulosic biomass to hydrocarbon fuels and coproducts: 2018 biochemical design case update; biochemical deconstruction and conversion of biomass to fuels and products via integrated biorefinery pathways, Report NREL/TP-5100-71949, National Renewable Energy Laboratory (U.S.), Golden, CO (United States), 2018. https://www.nrel.gov/docs/fy19osti/71949.pdf
5. Y. Liao, S.-F. Koelewijn, G. Van den Bossche, J. Van Aelst, S. Van den Bosch, T. Renders, K. Navare, T. Nicolai, K. Van Aelst, M. Maesen, H. Matsushima, J. M. Thevelein, K. Van Acker, B. Lagrain, D. Verboekend and B. F. Sels, *Science*, 2020, **367**, 1385-1390.
6. Alibaba, https://www.alibaba.com, (accessed Jun-12, 2020).
7. Intratec, https://www.intratec.us, (accessed Aug-13, 2020).
8. EIA, https://www.eia.gov/electricity/monthly/epm_table_grapher.php?t=epmt_5_03, (accessed Aug-13, 2020).
9. R. Davis, L. Tao, C. Scarlata, E. C. D. Tan, J. Ross, J. Lukas and D. Sexton, *NREL Tech. Rep.*, 2015, DOI: 10.2172/1176746.2015.